

# Nuclear Magnetic Resonance (NMR): Spectroscopy and Imaging

Toni Shiroka

April 7, 2014

**Abstract** Nuclear magnetic resonance (NMR) represents the selective absorption of electromagnetic radiation by nuclei with nonzero spin placed in an external magnetic field. When the field is kept fixed and strong RF pulses excite the sample, its response, the free induction decay - FID, delivers important information on static (line shape) and dynamic (relaxation time) properties. The dependence of NMR parameters on the nuclei surroundings, makes it a highly sensitive probe to the immediate environment and, hence, an extremely versatile spectroscopic tool. The vast and successful applications of NMR in the most disparate fields of science are witnessed by the many Nobel prizes in physics, chemistry, and medicine, awarded for work related to NMR.

## Contents

1 Objectives . . . . .	1
2 Introduction . . . . .	1
3 Basics of NMR . . . . .	2
4 Dynamics of an isolated spin . . . . .	3
5 Classical treatment of the variable-field effects . . . . .	4
6 Bloch equations . . . . .	5
7 Simple quantum theory of resonance . . . . .	7
8 Spin-lattice relaxation . . . . .	7
9 FT-NMR . . . . .	9
10 Magnetic resonance imaging (MRI) . . . . .	12
11 Measurement program . . . . .	12
A Measurement of self-diffusion coefficient . . . . .	13
B Some technical data of NMR spectrometer . . . . .	13
C Biographic notes . . . . .	13

## 1 Objectives

1. Understand the basics of NMR spectroscopy, its advantages and limits. Familiarize with the concepts of ro-

tating frame, transient response, radio-frequency pulse, resonant circuit, spin echo, etc.

2. Understand the concept of magnetic resonance and apply it to the case of nuclear spins in a magnetic field. Observe and interpret the NMR FID signal in a typical sample. Learn how to determine the  $90^\circ$  pulse length.
3. Learn how Fourier transform NMR works and how signal averaging is used to reveal the weak NMR signal. Estimate the amplitude of the induced voltage in a typical NMR experiment [3].
4. Understand the role of field gradients and how they can be used for imaging purposes. What determines the smallest gradient which can be used? Is field homogeneity important in this case and why?

## 2 Introduction

### 2.1 The history of NMR

The method of magnetic resonance was initially developed by I. Rabi in 1937 in order to measure the magnetic moment of neutron and, consequently, the moment of other nuclei. At that time molecular beams were used, which were made to deflect in an inhomogeneous magnetic field (after irradiation with a high-frequency signal). In this (rather complicated) way, the first nuclear-spin transitions could be detected.

The first magnetic resonance experiments in the solid state were carried out by E. Zavoisky, who could observe a strong electron-spin resonance (ESR) absorption in many paramagnetic salts.

The first nuclear-spin magnetic resonance (NMR) experiments in liquids and solids (water and paraffin, respectively), were carried out for the first time by Purcell, Torrey and Pound, as well as by Bloch, Hansen and Packard (both

in 1946). In 1952 Bloch and Purcell were awarded the Nobel prize for their ground-breaking work.

Already the early experiments in liquids hinted at the possibility that the method could detect even the slightest changes in the chemical environment of the probe nuclei, making NMR one of the preferred tools by the chemists.

The year 1966 marked another milestone in the history of NMR, when Anderson and Ernst managed to significantly improve the sensitivity of the method by the use of pulsed excitation and subsequent Fourier transform. This so-called Fourier-transform (or pulsed) NMR is currently the most common measurement method.

Finally, in 1973, Paul Lauterbur first and Peter Mansfield later, achieve the first images using the magnetic resonance imaging (MRI). Their discovery is awarded the Nobel prize in Medicine in 2003.

## 2.2 The measuring method

NMR is a highly developed, microscopic investigation technique, whereby the atomic nuclei of the substance being investigated act as its own probes. These probes interact with their environment (as, e.g., electrons, crystal fields, neighbouring nuclei, paramagnetic impurities, etc.), with consequent changes in their resonance frequency. By means of an NMR spectrometer this spectrum can be measured, then analyzed, and finally conclusions about the specific properties of the investigated substance can be drawn. NMR is capable of delivering information at an atomic scale. Since different types of interactions superimpose (which usually makes it difficult to observe the minor effects) new, refined NMR measurement methods have been and are being developed.

Currently, NMR is an established technique in many different fields, ranging from solid-state physics, to chemistry, biology, medicine, agriculture, archaeology, geology, etc. This implies a huge mass of books and publications on NMR, making the access to the technique rather overwhelming for the newcomer. Some of the most known textbooks are reported in the final bibliography.

## 3 Basics of NMR

### 3.1 The nuclear magnetic dipole moment

Most atomic nuclei have a magnetic dipole moment,  $\mu$ , due to their nuclear angular momentum  $\mathbf{J}$ .

$$\mathbf{J} = \hbar \mathbf{I} \quad (1)$$

where  $\mathbf{I}$  is the nuclear spin,  $I$  the spin quantum number (integer or half-integer), and  $\hbar$  is the reduced Planck constant. Depending on the number of protons and neutrons in the nucleus, the nuclear spin quantum number can vary.

**Table 1** Nuclear symmetry and spin.

Nucleus	Spin	Examples
even-even	$I = 0$	$I = 0$ : $^{12}\text{C}$ , $^{16}\text{O}$
odd-odd	$I \neq 0$ , integer	$I = 1$ : $^2\text{H}$ , $^6\text{Li}$ , $^{14}\text{N}$
odd-even	$I \neq 0$ , half-integer	$I = 1/2$ : $^1\text{H}$ , $^{13}\text{C}$ , ... $I = 3/2$ : $^{23}\text{Na}$ , $^{35}\text{Cl}$ , ...

The total angular momentum value is  $J = \hbar\sqrt{I(I+1)}$ , while its maximum component is  $\hbar I$ . In the nucleus the angular momenta of protons and neutrons combine to the total *angular* moment  $\mathbf{J}$ , which gives rise to the nuclear *magnetic* moment

$$\mu = \gamma \mathbf{J} = \gamma \hbar \mathbf{I} = g_I \mu_N \mathbf{I}, \quad (2)$$

where  $\gamma$  is the gyromagnetic ratio,  $g_I$  the nuclear  $g$ -factor,<sup>1</sup> and  $\mu_N = e\hbar/2m_p = 5.05 \times 10^{-27} \text{ Am}^2$  the nuclear magneton. The gyromagnetic ratios  $\gamma$  for different nuclei are known and tabulated. Differently from the excited states of atoms, which lie 1–100 eV above the atomic ground state, the excited states of a nucleus lie 0.01–10 MeV above the nuclear ground state. Therefore, at all effects the nuclear  $\gamma$  values are fixed and refer to the ground state of the nucleus. Notice that, although the proton and the neutron have the same spin-angular momentum as the electron,  $\hbar/2$ , their magnetic moments are far smaller since  $m_p = m_n = 1836 m_e$ .

### 3.2 Nuclear magnetization

When a collection of nuclear spins<sup>2</sup>  $I$ , is placed in a static magnetic field  $\mathbf{B}_0$ , the originally coinciding energy levels split into  $(2I + 1)$  distinct and equidistant states (nuclear Zeeman effect). The new levels,  $E_m = -m\hbar\omega_L$ , with  $\omega_L = \gamma B_0$  the Larmor precession frequency (see Sec. 7), depend on the applied field  $B_0$  and on the magnetic quantum number  $m$  [ $m = -I, -(I-1), \dots, I-1, I$ ].

In thermal equilibrium the different  $m$ -sub-levels are populated according to the Boltzmann distribution

$$P(E_m) \propto \exp(-E_m/k_B T). \quad (3)$$

Since the  $(2I + 1)$  energy states have different populations, on average each nucleus has a non-zero magnetic polarization:

$$\langle I_z \rangle = \frac{\sum_{m=-I}^I m \exp\left(-\frac{E_m}{k_B T}\right)}{\sum_{m=-I}^I \exp\left(-\frac{E_m}{k_B T}\right)}. \quad (4)$$

<sup>1</sup> For a nucleus  $g$  does not reflect the original meaning of the Landé  $g$ -factor as a spectroscopic line splitting, since the combination of intrinsic and orbital momenta is not known.

<sup>2</sup> Notice that often the nuclear spin is identified (although not correctly) with the nuclear magnetic moment.

For nuclear magnetic moments (at not too low temperatures) the energy splitting is tiny compared with the thermal energy,  $E_m \ll k_B T$ , therefore, one can use the approximation  $e^{-x} \approx 1 - x$ . By substituting  $E_m = -m\hbar\gamma B_0$  one obtains

$$\langle I_z \rangle = \frac{\sum_{m=-I}^I m \left(1 + \frac{\gamma\hbar m B_0}{k_B T}\right)}{\sum_{m=-I}^I \left(1 + \frac{\gamma\hbar m B_0}{k_B T}\right)}. \quad (5)$$

Since  $\sum_{m=-I}^I m = 0$ , the first term in the numerator and the second term in the denominator vanish, to obtain<sup>3</sup>

$$\langle I_z \rangle = \frac{\gamma\hbar B_0}{k_B T} \frac{\sum m^2}{2I+1} = \frac{\gamma\hbar I(I+1)B_0}{3k_B T}. \quad (6)$$

The value of nuclear spin polarization  $\langle I_z \rangle$  at room temperature ( $T \approx 300$  K) is quite small, e.g., for  $B_0 = 1$  T and  $I = 1$ ,  $\gamma\hbar = \mu_N$  and

$$\langle I_z \rangle = \frac{2}{3} \frac{\mu_N B_0}{k_B T} \approx 10^{-6}. \quad (7)$$

Despite the very small value of the latter, the unequal occupation of  $m$ -levels is crucial in observing the nuclear magnetic resonance. In fact, the nuclear spin polarization  $\langle I_z \rangle$  is closely related to the nuclear magnetization. The macroscopic magnetization  $\mathbf{M}$  of the atomic nuclei in a sample is the sum of the single moments  $\mu_i$  in a volume  $V$ , hence  $\mathbf{M} = \sum_i \mu_i / V$ . By using Eq. (2), the expectation value of the  $z$ -component of  $\mathbf{M}$  in the direction of the applied field  $\mathbf{B}_0$  has the following form:

$$M_z = \sum_i \mu_{i,z} / V = N\gamma\hbar \langle I_z \rangle, \quad (8)$$

where  $N$  is the concentration of the nuclei. By substituting  $\langle I_z \rangle$  from Eq. (6) one obtains the nuclear magnetization value at thermal equilibrium:

$$M_0 = N \frac{\gamma^2 \hbar^2 I(I+1)}{3k_B T} B_0. \quad (9)$$

On the other hand, one can express the macroscopic magnetization  $M_0$  by using the nuclear-spin susceptibility  $\chi_N$  and the magnetic field intensity  $H_0 (= B_0/\mu_0)$  as  $M_0 = \chi_N H_0$ . A comparison with the previous formula for  $M_0$  gives, therefore, the nuclear-spin susceptibility:

$$\chi_N = \mu_0 \frac{N\gamma^2 \hbar^2 I(I+1)}{3k_B T} = \frac{\text{const.}}{T} \quad (\text{Curie law}) \quad (10)$$

#### 4 Dynamics of an isolated spin — classical approach

Classically a magnetic dipole moment  $\mu$  in an applied field  $\mathbf{B}$  experiences a torque  $\mathbf{D} = \mu \wedge \mathbf{B}$ . If it possesses also angular momentum about the dipolar axis, i.e.,  $\mu = \gamma \mathbf{J}$ , then it will tend to precess about the instantaneous magnetic field. Indeed, since  $\mathbf{D} = d\mathbf{J}/dt$ , one has

$$\frac{d\mu}{dt} = \mu \wedge (\gamma \mathbf{B}) \quad (\text{spin precession}) \quad (11)$$

Preferentially we use a rotating coordinate system, since there the equation of motion is particularly simple.<sup>4</sup>

An arbitrary vector  $\mathbf{F}(t)$  can be written in the form  $\mathbf{F}(t) = \mathbf{e}_x F_x + \mathbf{e}_y F_y + \mathbf{e}_z F_z$ , where  $\mathbf{e}_x$ ,  $\mathbf{e}_y$ ,  $\mathbf{e}_z$  and  $F_x$ ,  $F_y$ ,  $F_z$  are functions of time.

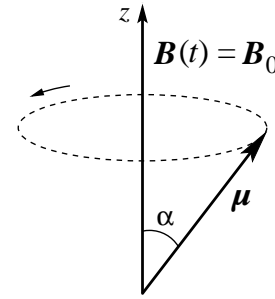


Fig. 1 When the field  $\mathbf{B}$  is constant the angle  $\alpha$  is constant, too.

Let a coordinate system rotate with an angular velocity  $\Omega$ :

$$\frac{d\mathbf{e}_x}{dt} = \Omega \wedge \mathbf{e}_x; \quad \frac{d\mathbf{e}_y}{dt} = \Omega \wedge \mathbf{e}_y; \quad \frac{d\mathbf{e}_z}{dt} = \Omega \wedge \mathbf{e}_z; \quad (12)$$

The time derivative of an arbitrary vector  $\mathbf{F}(t)$  can then be written as

$$\frac{d\mathbf{F}}{dt} = \frac{\delta \mathbf{F}}{\delta t} + \Omega \wedge \mathbf{F} \quad (13)$$

where, by definition

$$\frac{\delta \mathbf{F}}{\delta t} := \mathbf{e}_x \frac{dF_x}{dt} + \mathbf{e}_y \frac{dF_y}{dt} + \mathbf{e}_z \frac{dF_z}{dt}, \quad (14)$$

with  $\frac{\delta}{\delta t}$  representing the time derivative in the rotating system. For the equation of motion (11) this gives

$$\frac{d\mu}{dt} = \frac{\delta \mu}{\delta t} + \Omega \wedge \mu = \mu \wedge (\gamma \mathbf{B}) \quad (15)$$

$$\frac{\delta \mu}{\delta t} = \mu \wedge (\gamma \mathbf{B} + \Omega) \quad (16)$$

<sup>4</sup> A derivation of the equation of motion in a rotating frame of reference by means of linear algebra can be found, e.g., in Ref. [13].

<sup>3</sup>  $\sum_{m=-I}^I m^2 = (2I+1)I(I+1)/3$

From the last equation it is clear that  $\mu$  moves in the rotating system as it does in the laboratory system, except that  $\mathbf{B}$  must be replaced by the effective field  $\mathbf{B}_{\text{eff}} = \mathbf{B} + \frac{\Omega}{\gamma}$ .

If  $\mathbf{B} = B_0 \mathbf{e}_z$ , one can choose  $\Omega = -\gamma B_0 \mathbf{e}_z$ , so that  $\mathbf{B}_{\text{eff}} = 0$  and, therefore,  $\frac{\delta \mu}{\delta t} = 0$ . The rotation frequency  $\gamma B_0 / 2\pi$  is known as the *Larmor frequency*.

Independent of the evolution in time of  $\mathbf{B}(t)$ , the magnitude of  $\mu$  is a constant of motion. Indeed, from the equation of motion (11) it follows that  $\mu \perp \frac{d\mu}{dt}$  from which one has

$$\frac{d(\mu^2)}{dt} = 2\mu \frac{d\mu}{dt} = 0. \quad (17)$$

## 5 Classical treatment of the variable-field effects

$\mathbf{B}_0 = (0, 0, B_0)$ ;  $\mathbf{B}_1(t) = (2B_1 \cos \omega t, 0, 0)$ , where  $\mathbf{B}_1$  is obtained through the superposition of two fields, one left- and one right-rotating,  $\mathbf{B}_{1l}$  and  $\mathbf{B}_{1r}$ , respectively.

$$\mathbf{B}_{1l} + \mathbf{B}_{1r} = B_1 (\mathbf{e}_x^L \cos \omega t + \mathbf{e}_y^L \sin \omega t) + B_1 (\mathbf{e}_x^L \cos \omega t - \mathbf{e}_y^L \sin \omega t), \quad (18)$$

where the upper index  $L$  indicates the laboratory system, whereas the absence of an index indicates the rotating system. From now on we will consider only one of the rotating components and denote its angular speed with  $\omega_z$ , which can be of either sign.<sup>5</sup> With this notation we have  $\mathbf{B}_1(t) = B_1 (\cos \omega_z t, \sin \omega_z t, 0)$ .

The equation of motion of spin (11) can now be written

$$\frac{d\mu}{dt} = \mu \wedge \gamma [\mathbf{B}_0 + \mathbf{B}_1(t)]. \quad (19)$$

In the rotating frame system, which rotates with  $\omega_z$  around the  $z$ -axis, one can write

$$\frac{\delta \mu}{\delta t} = \mu \wedge [\mathbf{e}_z (\omega_z + \gamma B_0) + \mathbf{e}_x \gamma B_1] \quad (20)$$

and, if we choose  $\omega_z = -\omega$ , then

$$\boxed{\frac{\delta \mu}{\delta t} = \mu \wedge \gamma \left[ \mathbf{e}_z \left( B_0 - \frac{\omega}{\gamma} \right) + \mathbf{e}_x B_1 \right] = \mu \wedge (\gamma \mathbf{B}_{\text{eff}})} \quad (21)$$

$$\text{with } \mathbf{B}_{\text{eff}} = \mathbf{e}_z \left( B_0 - \frac{\omega}{\gamma} \right) + \mathbf{e}_x B_1.$$

<sup>5</sup> This is allowed since the sense of rotation can be fixed also a posteriori.

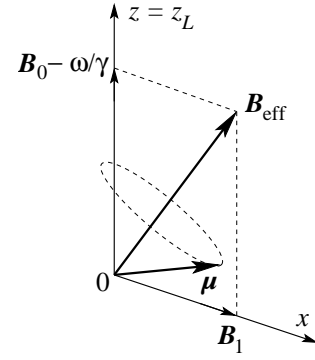


**Fig. 2** Precession of the nuclear magnetic moment  $\mu$  around  $\mathbf{B}_{\text{eff}}$  in the rotating frame of reference.

In the rotating frame  $\mu$  precesses around  $\mathbf{B}_{\text{eff}}$  (see Fig. 2). The  $z$ -component of  $\mu$  moves up and down, although no energy is being absorbed. Therefore, the sign of  $(B_0 - \omega/\gamma)$  can be either positive or negative.

In resonance, i.e., for  $\omega = \gamma B_0$ , the  $z$ -component of  $\mathbf{B}_{\text{eff}}$  vanishes. Hence, in this case  $\mathbf{B}_{\text{eff}} = \mathbf{B}_1$  and the rotation angle of  $\mu$  is  $\alpha = \gamma B_1 t_p$ , where  $t_p$  is the duration of a pulse of the additional field  $\mathbf{B}_1(t)$ .

In deriving Eq. (21) in the rotating frame of reference, the component rotating at  $2\omega$  was ignored. This can be done since the effects related to the  $2\omega$ -term can be safely neglected. Classically, this can be understood by considering that the  $2\omega$ -term vibrates almost at  $\mathbf{B}_{\text{eff}}$  with a high frequency  $2\omega$ , but with a very small amplitude (since  $B_1 \ll B_0$ ). On average, therefore, the effect of this term can be neglected.

## Observation of NMR

The above considerations suggest a very simple method for observing the nuclear magnetic resonance (NMR). One can insert the material to be investigated in a coil, whose axis is orthogonal to the  $\mathbf{B}_0$  field. In thermal equilibrium, a macroscopic magnetization will build up along the direction of the applied field. By applying an alternating voltage with frequency  $\omega$  for a duration  $t_p$  one can generate an alternating field  $B_1$  orthogonal to  $B_0$ . By an appropriate choice of  $B_1$  and  $t_p$  it is possible to rotate the magnetization by an angle  $\alpha = 90^\circ$ , so as to bring it perpendicular to  $B_0$ . In this case, the magnetization will precess with the frequency  $\gamma B_0$  around  $\mathbf{B}_0$  thus generating an alternating magnetic flux in the coil. The resulting induced voltage (Faraday law) can then be amplified and observed.

According to the above presentation, the NMR signal would last forever. However, the interactions of the nuclear spins with their environment will gradually damp the signal

which, therefore, is appropriately named *free induction decay*, FID (here “free” means in the absence of the exciting  $B_1$  field). Typical decay times of the FID are from some ms to some seconds in liquids, but only ca. 100  $\mu$ s in solids.

## 6 Bloch equations

Bloch found that the motion of macroscopic nuclear magnetization  $\mathbf{M}$  in a magnetic field  $\mathbf{B}$  can be described phenomenologically by a set of differential equations. The starting point for writing the *Bloch equations* is the classical motion of a magnetic dipole in a magnetic field. Since the macroscopic magnetization  $\mathbf{M}$  is the sum of nuclear magnetic dipole moments, from Eq. (11) one can write

$$\frac{d\mathbf{M}}{dt} = \gamma(\mathbf{M} \wedge \mathbf{B}). \quad (22)$$

The laboratory system has  $\{\mathbf{e}_x^L, \mathbf{e}_y^L, \mathbf{e}_z^L\}$  as basis vectors and  $\{x_L, y_L, z_L\}$  as vector components, while for the rotating system these are  $\{\mathbf{e}_x, \mathbf{e}_y, \mathbf{e}_z\}$  and  $\{x, y, z\}$ , respectively, with  $\mathbf{e}_z^L \parallel \mathbf{e}_z$  (we choose  $\mathbf{B}$  parallel to  $\mathbf{e}_z^L$  direction). In thermal equilibrium the magnetization and the magnetic field are parallel to each other. Hence, the equilibrium magnetization contains only one component,  $M_z = M_0$ .

Every system tends to reach an equilibrium state. If one assumes that the speed with which this state is reached is proportional to the deviation from the equilibrium, then this assumption implies the following *Bloch equations*

$$\begin{aligned} \frac{dM_{xL}}{dt} &= \gamma(\mathbf{M} \wedge \mathbf{B})_{xL} - \frac{M_{xL}}{T_2} \\ \frac{dM_{yL}}{dt} &= \gamma(\mathbf{M} \wedge \mathbf{B})_{yL} - \frac{M_{yL}}{T_2} \\ \frac{dM_{zL}}{dt} &= \gamma(\mathbf{M} \wedge \mathbf{B})_{zL} + \frac{M_0 - M_{zL}}{T_1} \end{aligned} \quad (23)$$

or in vectorial form

$$\frac{d\mathbf{M}_L}{dt} = \gamma(\mathbf{M} \wedge \mathbf{B})_L - \frac{M_x \mathbf{e}_x^L + M_y \mathbf{e}_y^L}{T_2} - \frac{M_z - M_0}{T_1} \mathbf{e}_z^L. \quad (24)$$

$T_1$  represents the so-called longitudinal relaxation time, known also as the *spin-lattice* relaxation time. It is a measure of how fast the energy is exchanged between the nuclear spin system and its surroundings, the so-called *lattice*. In solids  $T_1$  can have very different values, from some  $\mu$ s up to thousands of seconds.

$T_2$  is known as the transverse relaxation time or *spin-spin* relaxation time. It describes how fast the transverse components of the nuclear magnetic moments de-phase. One of the main reasons why in solids the nuclear-spin ensemble

loses its phase coherence is the nuclear dipole interaction. In this case, one can roughly estimate  $T_2$  by using:

$$\frac{1}{\gamma B_{\text{local}}} \simeq \frac{4\pi r^3}{\mu_0 \gamma^2 \hbar} \approx 100 \mu\text{s}. \quad (25)$$

### 6.1 Solution of Bloch equations for small $B_1$ fields

We consider now a frame system  $\{x, y, z\}$  rotating with an angular speed  $-\omega$  around  $\mathbf{B}_0 \parallel \mathbf{e}_z^L \parallel \mathbf{e}_z$  and choose  $\mathbf{B}_1 \parallel \mathbf{e}_x$ . The magnetic induction in the rotating frame is then  $\mathbf{B}_{\text{eff}} = (B_1, 0, h_0)$ , with  $h_0 = B_0 - \omega/\gamma$ . By substituting the field components in the Bloch equations (24) one obtains:

$$\begin{aligned} \frac{dM_x}{dt} &= \gamma M_y h_0 - \frac{M_x}{T_2} \\ \frac{dM_y}{dt} &= \gamma(M_z B_1 - M_x h_0) - \frac{M_y}{T_2} \\ \frac{dM_z}{dt} &= -\gamma M_y B_1 + \frac{M_0 - M_z}{T_1} \end{aligned} \quad (26)$$

In a stationary state one can write that  $\frac{dM_z}{dt} = 0$ , from which it follows that  $M_y = \frac{M_0 - M_z}{\gamma B_1 T_1}$ . When  $B_1 \rightarrow 0$ , both  $M_y$  and  $M_x$  should in any case vanish, i.e.,  $M_0 - M_z$  should tend to zero faster than  $B_1$ . However, since  $B_1$  has to be small, one can substitute  $M_z$  with  $M_0$  in the second of Eqs. (26), which simplifies significantly the solution of the equations. Further, by introducing the terms  $M_+ := M_x + iM_y$  and  $\alpha := 1/T_2 + i\gamma h_0$  the first two equations can be written:

$$\frac{dM_+}{dt} = -\alpha M_+ + i\gamma M_0 B_1 \quad (27)$$

whose solution is

$$M_+ = A e^{-\alpha t} + \frac{i\gamma M_0 B_1}{1/T_2 + i\gamma h_0} \quad (28)$$

Since we are interested in a stationary solution, the first term in Eq. (28) can be neglected, as it represents a (time-decaying) transient. Then, by using  $M_0 = \chi_0 B_0 / \mu_0$ , and  $\omega_0 = \gamma B_0$  one finally obtains

$$\begin{aligned} M_+ &= \frac{i\gamma(\chi_0/\mu_0)B_0 B_1 T_2}{1 + iT_2(\omega_0 - \omega)} \\ M_x &= \frac{\chi_0}{\mu_0} \omega_0 T_2 \frac{(\omega_0 - \omega)T_2}{1 + (\omega_0 - \omega)^2 T_2^2} B_1 \\ M_y &= \frac{\chi_0}{\mu_0} \omega_0 T_2 \frac{1}{1 + (\omega_0 - \omega)^2 T_2^2} B_1 \end{aligned} \quad (29)$$

$M_x$ ,  $M_y$  and  $M_z$  do not depend on time in the rotating frame system, implying the same for the macroscopic magnetization there. In the fixed laboratory system  $\{x_L, y_L, z_L\}$ ,

however, they rotate with an angular speed  $\omega$ . In a typical experiment we observe this rotating magnetization, which induces a voltage in a fixed coil in the laboratory system. If the coil is oriented, e.g., along the  $x_L$ -direction, then we can calculate the oscillating magnetization component along  $x_L$

$$M_{x_L}(t) = M_x \cos \omega t + M_y \sin \omega t \quad (30)$$

The alternating magnetic field applied to the coil (now described as an  $H$ -field) is

$$H_{x_L}(t) = \frac{2B_1}{\mu_0} \cos \omega t = 2H_{1x} \cos \omega t \quad (31)$$

Since  $M_{x_L}$  and  $M_{y_L}$  are proportional to  $B_1$  and, hence, also to  $H_{1x}$ , we can write Eq. (30) as

$$M_{x_L}(t) = (\chi' \cos \omega t + \chi'' \sin \omega t) H_{1x}. \quad (32)$$

By a comparison with  $M_x$  and  $M_y$  from Eq. (29) we obtain:

$$\chi'(\omega) = \frac{\chi_0}{2} \omega_0 T_2 \frac{(\omega_0 - \omega) T_2}{1 + (\omega_0 - \omega)^2 T_2^2} = K \frac{\eta}{1 + \eta^2} \quad (33)$$

$$\chi''(\omega) = \frac{\chi_0}{2} \omega_0 T_2 \frac{1}{1 + (\omega_0 - \omega)^2 T_2^2} = K \frac{1}{1 + \eta^2}, \quad (34)$$

where  $K = \frac{\chi_0}{2} \omega_0 T_2$  and  $\eta = (\omega_0 - \omega) T_2$ . These resonance line shapes are known as *Lorentzian* lines (see Fig. 3).

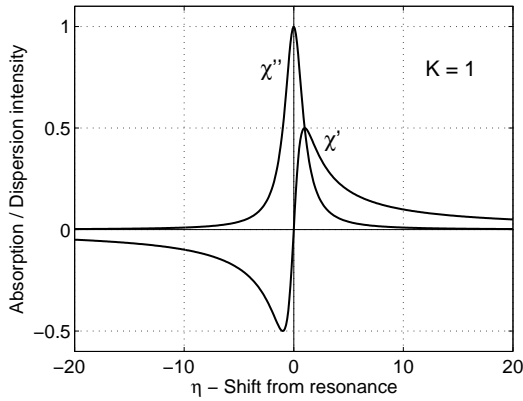


Fig. 3 Real  $\chi'(\omega)$  and imaginary  $\chi''(\omega)$  parts of the susceptibility.

The relation between  $M_{x_L}$  and the applied field  $H_{x_L}(t)$  can be conveniently written in a complex form. By using  $M_{x_L}^c(t) = \chi H_{x_L}^c(t)$ , where  $\chi = \chi' - i\chi''$  and  $H_{x_L}^c(t) = H_{1x_L} e^{i\omega t}$ , one obtains

$$M_{x_L}(t) = \text{Re} \{ \chi H_{1x_L} e^{i\omega t} \} \quad (35)$$

Better yet, one can consider  $\chi$  as a tensor, which implies that, e.g., one can obtain a magnetization component along

the  $\mathbf{e}_y$ -direction even by applying a magnetic field along the  $\mathbf{e}_x$ -direction. Hence, generally we can write:

$$M_{\alpha}^c(t) = \chi_{\alpha\beta} H_{\beta 0} e^{i\omega t}, \quad \text{where } \alpha, \beta = x_L, y_L, z_L. \quad (36)$$

The deduced  $\chi$  values of interest to us are  $\chi_{x_L x_L}$  (the contribution from  $\chi$  in the  $(xy)_L$ -plane remains constant,  $|\chi_{x_L x_L}| = |\chi_{x_L y_L}|$ ).

Although the relation between magnetization and the applied field was obtained via the Bloch equations, the dependence itself is quite general. Indeed, every resonance phenomenon is characterized by a complex susceptibility, which expresses the same relation between excitation and response.

Let us now consider the *power absorbed* by the nuclear spins. We have a coil filled with material on which we observe nuclear magnetic resonance. The coil inductivity is  $L = \mu L_0$  with  $\mu = 1 + \chi(\omega)$  and the impedance  $Z = i\omega L + R_0 = i\omega L_0(1 + \chi') + \omega L_0 \chi'' + R_0$ . The relative change of resistance, caused by the material in the coil, is therefore

$$\frac{\Delta R}{R_0} = \frac{\omega L_0}{R_0} \chi'' = \chi'' Q. \quad (37)$$

Here  $Q$  is the quality factor of the empty coil. In the absence of a sample the maximum energy stored in the coil is

$$\frac{1}{2} L_0 i_0^2 = \frac{\mu_0 H_1^2}{2} V = \frac{B_1^2}{2\mu_0} V. \quad (38)$$

Nuclear spins absorb on average the power  $\bar{P}$ :

$$\bar{P} = \frac{1}{2} i_0^2 \Delta R = \frac{1}{2} i_0^2 L_0 \omega \chi'' = \frac{B_1^2}{2\mu_0} \chi'' V \quad (39)$$

This relation associates in a simple way the absorbed power, the susceptibility  $\chi''$ , and the applied field. Later on we will use it as a starting point for calculating  $\chi''$  at a microscopic level, since the *absorbed power can be calculated by means of the transition probability*. If  $\chi''(\omega)$  is known, then also the other term  $\chi'(\omega)$  is known. This is because both of them are related via the very generally valid *Kramers-Kronig relations* (here  $P$  represents the *principal value* of a function):

$$\chi'(\omega) - \chi'(\infty) = \frac{1}{\pi} P \int_{-\infty}^{\infty} \frac{\chi''(\omega')}{\omega' - \omega} d\omega', \quad (40)$$

$$\chi''(\omega) = -\frac{1}{\pi} P \int_{-\infty}^{\infty} \frac{\chi'(\omega') - \chi'(\infty)}{\omega' - \omega} d\omega'.$$

## 7 Simple resonance theory — quantum-mechanical approach

Let us consider first the quantum mechanical description of a nuclear magnetic moment in an external field  $\mathbf{B}$ . The Hamiltonian operator is:

$$\mathcal{H} = -\boldsymbol{\mu} \cdot \mathbf{B} = -\gamma \hbar \mathbf{I} \cdot \mathbf{B}. \quad (41)$$

By considering  $\mathbf{B}$  along the  $z$ -axis,  $\mathbf{B} = (0, 0, B_0)$ , it follows

$$\mathcal{H} = -\gamma \hbar B_0 I_z = -\hbar \omega_0 I_z. \quad (42)$$

The energy eigenvalues of  $\mathcal{H}$  are  $E_m = -\hbar \omega_0 m$ . We obtain therefore  $2I + 1$  equidistant energy levels, each  $\Delta E = \hbar \omega_0 = \gamma \hbar B_0$  apart from the other (see Fig. 4).

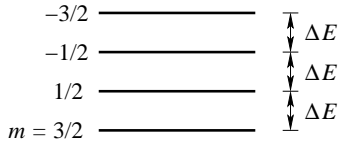


Fig. 4 Energy levels of a nuclear spin  $I = 3/2$  in a magnetic field.

To observe the resonance we need an interaction capable of promoting transitions between the different energy levels. Because of the energy-conservation law, this interaction has to be time-dependent with an angular frequency  $\omega$  such that  $\hbar \omega = \Delta E = \hbar \omega_0$ . Moreover, the interaction should have a non-vanishing matrix element which connects the initial and the final states. Usually an oscillating magnetic field  $\mathbf{B}_1(t) \perp \mathbf{B}_0$ , with  $\mathbf{B}_1(t) = (B_1 \cos(\omega t), 0, 0)$  is used. Its Hamiltonian operator can then be written:

$$\mathcal{H} = -\gamma \hbar B_1 I_x \cos(\omega t). \quad (43)$$

Since  $\langle m | I_x | m+1 \rangle \neq 0$ , we can only have transitions between neighbouring levels, i.e.,  $\hbar \omega = \Delta E = \hbar \omega_0$  and hence  $\omega = \gamma B_0$ . Since Planck's constant does not appear in the resonance relation, it suggests that the same result should still be valid also in a classical approach.

A simple classical picture can help us estimate the order of magnitude of  $\gamma$ . Let us consider a particle with mass  $m$  and charge  $e$ , which circulates with a period  $T$  on a circular path with radius  $r$ .

The angular momentum of the particle is  $J = mvr = m \frac{2\pi r^2}{T}$  and it gives rise to a circular current  $i = \frac{e}{T}$ . For the magnetic dipole moment one has  $\boldsymbol{\mu} = i\pi r^2 = \frac{e\pi r^2}{T}$ , from which we obtain the gyromagnetic ratio:  $\gamma = \frac{\boldsymbol{\mu}}{J} = \frac{e}{2m}$ .

In general, a large mass implies a small magnetic dipole moment. From  $\omega = \gamma B_0$ , in an applied field  $B_0 = 1$  T we have:

$$\underbrace{\omega(\text{Electron Spin Resonance})}_{10 \text{ GHz}} \gg \underbrace{\omega(\text{NMR})}_{10 \text{ MHz}} \quad (44)$$

## 8 Energy absorption and spin-lattice relaxation

For the sake of convenience, in the following let us consider  $I = 1/2$ . One can write:

$$\mathcal{H} = -\boldsymbol{\mu} \cdot \mathbf{B} = -\gamma \hbar B_0 I_z, \quad E_m = -\hbar \omega_0 m \quad \text{and} \quad \omega_0 = \gamma B_0.$$

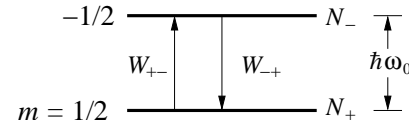


Fig. 5 Quantum transitions in a nuclear spin-1/2 system.

If the occupation numbers for the energy levels are  $N_+$  and  $N_-$  and the transition probabilities  $W_{-+}$  and  $W_{+-}$ , respectively (see Fig. 5), then the rate of change of the occupation number  $N_+$  is

$$\frac{dN_+}{dt} = N_- W_{-+} - N_+ W_{+-} \quad (45)$$

If we suppose now that an external perturbation  $\mathcal{H}_{\text{pert}} \propto B_1 \cos(\omega t)$  acts on the system, it will induce transitions between the energy levels. The transition probability between two such states can be calculated by means of the *Fermi's golden rule*:

$$W_{+-} = \frac{2\pi}{\hbar} |\langle - | \mathcal{H}_{\text{pert}} | + \rangle|^2 \underbrace{\delta(E_+ - E_- - \hbar \omega)}_{\text{Energy conservation}} \propto B_1^2 \quad (46)$$

Since  $|\langle - | \mathcal{H}_{\text{pert}} | + \rangle|^2 = |\langle + | \mathcal{H}_{\text{pert}} | - \rangle|^2$ , then  $W_{+-} = W_{-+} =: W$  and, consequently

$$\frac{dN_+}{dt} = W(N_- - N_+). \quad (47)$$

By introducing  $n = N_+ - N_-$  and  $N = N_+ + N_-$ , we have  $N_+ = \frac{1}{2}(N + n)$  and  $N_- = \frac{1}{2}(N - n)$ , from which we obtain:

$$\frac{dN_+}{dt} = -Wn \quad (48)$$

$$\frac{dN_-}{dt} = +Wn$$

and consequently

$$\left(\frac{dn}{dt}\right)_{\text{HF}} = -2Wn \quad (49)$$

whose solution is  $n(t) = n(0) \exp(-2Wt)$ , with  $\lim_{t \rightarrow \infty} n(t) = 0$ . Hence, the resulting energy absorption is:

$$\frac{dE}{dt} = N_+ W \hbar \omega - N_- W \hbar \omega = \hbar \omega W n. \quad (50)$$

As  $n$  goes towards zero with time, the energy absorption will gradually cease and no resonance would be observed.

If a piece of material is brought into a static magnetic field (or taken out of it) without applying any oscillating magnetic field ( $W = 0$ ), the material will be magnetized or demagnetized, respectively. According to the last equation this would not be possible, since for  $W = 0$  also  $dN_+/dt = dN_-/dt = 0$ , hence no change in the occupation numbers would be possible.

However, the process of (de)magnetization requires transitions between the energy levels, i.e., the spin system should be coupled to a thermal reservoir with which it can exchange energy. The ratio  $N_-^0/N_+^0$  reflects the temperature of the thermal bath, since

$$\frac{N_-^0}{N_+^0} = \exp\left(-\frac{\Delta E}{k_B T}\right) = \exp\left(-\frac{\hbar \omega_0}{k_B T}\right). \quad (51)$$

We should postulate a mechanism which can induce transitions between the energy levels. We indicate by  $W_\uparrow$  the probability of the  $+ \rightarrow -$  transition and by  $W_\downarrow$  that of the  $- \rightarrow +$  transition.

We have then  $dN_+/dt = N_- W_\downarrow - N_+ W_\uparrow$ . Since in a stationary state  $dN_+/dt = 0$ , it follows that

$$\frac{N_-^0}{N_+^0} = \frac{W_\uparrow}{W_\downarrow} \implies \frac{W_\downarrow}{W_\uparrow} = \exp\left(+\frac{\hbar \omega_0}{k_B T}\right). \quad (52)$$

Before we had  $W_{+-} = W_{-+}$ . How it is that now  $W_\uparrow \neq W_\downarrow$ ? This apparent paradox can be solved by taking into account that a thermal transition in a spin system does not require only a coupling to the thermal bath, but also the existence of energy states (of the bath) that allow such a transition. The transition rate, therefore, will depend not only on the matrix element of the perturbation, but also on the probability that the reservoir is in a state that allows such a transition (see Fig. 6).

Since in a stationary state  $N_1 N_b W_{1b \rightarrow 2a} = N_2 N_a W_{2a \rightarrow 1b}$  and from quantum mechanics it is known that  $W_{2a \rightarrow 1b} = W_{1b \rightarrow 2a}$ , we have

$$\frac{N_1}{N_2} = \frac{N_a}{N_b} = \frac{W_\uparrow}{W_\downarrow}, \quad \text{where} \quad \begin{cases} W_\uparrow = N_a W_{2a \rightarrow 1b} \\ W_\downarrow = N_b W_{1b \rightarrow 2a} = N_b W_{2a \rightarrow 1b} \end{cases}$$

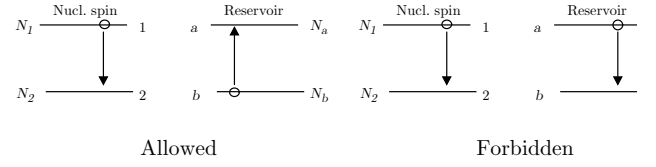


**Fig. 6** A thermal transition in the spin system can take place only if the heat reservoir can absorb the released energy.

The rate of change of the occupation numbers can be written as:

$$\frac{dN_+}{dt} = N_- W_\downarrow - N_+ W_\uparrow \quad \text{and} \quad \frac{dN_-}{dt} = N_+ W_\uparrow - N_- W_\downarrow \quad (53)$$

and, hence:

$$\frac{dn}{dt} = 2N_- W_\downarrow - 2N_+ W_\uparrow = N(W_\downarrow - W_\uparrow) - n(W_\downarrow + W_\uparrow). \quad (54)$$

With the newly defined quantities

$$n_0 := N \frac{W_\downarrow - W_\uparrow}{W_\downarrow + W_\uparrow} \quad \text{and} \quad \frac{1}{T_1} := W_\downarrow + W_\uparrow$$

the final result is

$$\left(\frac{dn}{dt}\right)_{\text{thermal}} = \frac{n_0 - n}{T_1}. \quad (55)$$

Here  $T_1$  represents the *spin-lattice relaxation time*, which we already know from the Bloch equation, while  $n_0$  is the difference in the occupation numbers at thermal equilibrium. The solution of the above differential equation is

$$n(t) = n_0 + A \cdot \exp\left(-\frac{t}{T_1}\right). \quad (56)$$

By including now the effects of both the high-frequency field (49) and that of the thermal processes (55) we obtain:

$$\frac{dn}{dt} = \left(\frac{dn}{dt}\right)_{\text{HF}} + \left(\frac{dn}{dt}\right)_{\text{thermal}} = -2Wn + \frac{n_0 - n}{T_1} \quad (57)$$

In a stationary state ( $dn/dt = 0$ ) we have that  $n = \frac{n_0}{1 + 2WT_1}$  which, for  $2WT_1 \ll 1$ , implies  $n \approx n_0$ .

The absorbed power can finally be calculated as

$$\frac{dE}{dt} = n \hbar \omega W = n_0 \hbar \omega \frac{W}{1 + 2WT_1}, \quad (58)$$

where  $W \propto B_1^2$  [see Eq. (46)]. For  $W > 1/(2T_1)$  we observe a saturation. From the behaviour of saturation one can estimate the spin-lattice relaxation time  $T_1$ , which depends on

microscopic process in the material. The absorption rate is related to  $W$ . An estimate of the resonant absorption is essential in establishing whether the resonance can be observed or not.

The energy levels are not perfectly sharp. Additional internal fields always present in matter will broaden the levels and, hence, the resonance line. The study of line widths provides further crucial information on the microscopic properties of the investigated substance.

## 9 Fourier-transform nuclear magnetic resonance

By applying a high-frequency magnetic field  $B_1$ , the magnetization can be tipped away from the initial  $\mathbf{e}_z$  direction. The particular case, in which  $B_1$  has exactly the Larmor frequency, is shown in Fig. 7 (left panel). In this case,  $\mathbf{B}_{\text{eff}} = \mathbf{B}_1$  and the magnetization (in the rotating frame) precesses around the  $\mathbf{e}_x$ -axis. The precession angle is  $\alpha = \gamma B_1 t_p$ , with  $t_p$  the HF pulse duration. It is clear, that by choosing the pulse duration one can obtain any HF precession angle.

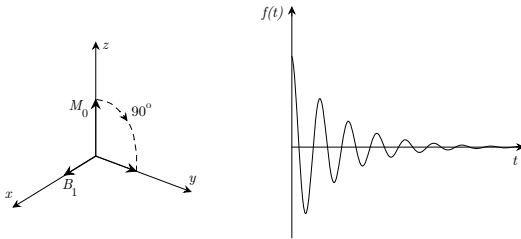


**Fig. 7** 90° pulse for the case when  $B_1$  is irradiated at the Larmor frequency (left) and the subsequent free-induction decay (right).

For technical reasons the amplitude  $B_1$  of the RF pulse is considerably smaller than that of the static field  $B_0$ . It can be shown that this does not represent an important constraint as long as

$$\gamma B_1 \gg \Delta \omega \quad (\text{= spectral width}) \quad \text{and} \quad \gamma B_1 \gg |\omega - \omega_0| \quad (59)$$

or, equivalently, that the pulse duration  $t_p$  is chosen so that

$$t_p \Delta \omega \ll 1 \quad \text{and} \quad t_p (\omega - \omega_0) \ll 1. \quad (60)$$

These conditions have the following meaning:

$t_p \Delta \omega \ll 1$ : In the rotating system the magnitude of  $B_{\text{eff}}$  is the same for all the components of magnetization over the whole spectral range  $\Delta \omega$ , i.e. they will be rotated by the same angle.

$t_p (\omega - \omega_0) \ll 1$ : The phase error remains possibly small.

After a 90° pulse the magnetization, initially pointing along the  $\mathbf{e}_z$  direction, will point in the  $\mathbf{e}_y$  direction. Once the RF field is switched off, the magnetization will precess freely in the  $(xy)_L$  plane and gradually will revert to its initial equilibrium state by means of  $T_1$ - and  $T_2$ -relaxation processes. This so-called free induction decay, *FID*, is shown in Fig. 7 (right panel).

To observe the precession of the macroscopic magnetization we use a fixed receiving coil, which is used also for exciting the sample. To estimate the voltage induced in the receiving coil we use the same expressions employed for the continuous RF field (Bloch equations). There is, though, an essential distinction between this and the continuous RF-field method: while in the latter the single resonance lines are scanned consecutively by varying the RF frequency (or, equivalently, the  $B_0$  field value), in the pulsed NMR method the different precession frequencies are observed simultaneously. Nowadays, pulsed NMR is practically the only method in common use.

If the nuclei in the sample sense different static fields (as the sum of a constant external field  $B_0$  with different inner fields), also  $B_{\text{eff}}$ , the effective field in the rotating system, will differ according to the nucleus location. Only for certain fraction of nuclei  $\mathbf{B}_{\text{eff}} = \mathbf{B}_1$  and only these nuclei will rotate by exactly 90° during  $t_p$ . The other nuclear spins will not end up in the  $(xy)_L$  and will only partially contribute to the free induction decay signal. In order that all nuclei fully participate to the FID, the condition  $|\omega_L - \omega| \ll \gamma B_1$  must be satisfied. This means that the angle between  $\mathbf{B}_{\text{eff}}$  and  $\mathbf{B}_1$  should be quite small.

By performing a Fourier transform of the time-domain spectrum one obtains the underlying frequencies and their line widths (see Fig. 8). Since in pulsed NMR one works in the frequency domain, the technique is commonly known as *Fourier-Transform-NMR (FT-NMR)*.

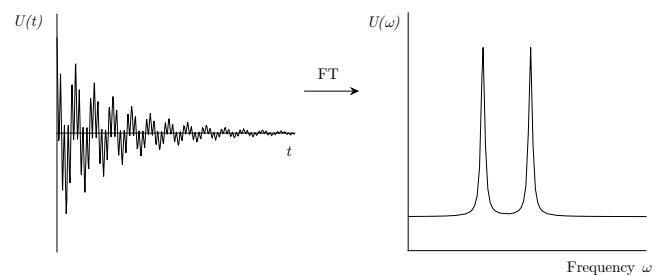


**Fig. 8** NMR signal in time domain and its absorption spectrum in the frequency domain, as obtained by a Fourier transform.

The simultaneous observation of several NMR lines is very advantageous in terms of statistics. In fact, differently from the continuous case, in pulsed NMR much more information can be collected in the same amount of time. However, the crucial advantage of pulsed NMR consists in its

multiple application possibilities, achievable through the use of specific pulse sequences (*multi-pulse methods*). As an example, in the following section we will discuss the spin-echo method.

### 9.1 Instrumentation for the FT-NMR method

In a complex NMR spectrum with many resonance lines the FID signal consists of a sum of oscillating components  $M_{xL}(t)$ , which decay over time due to line broadening processes. Generally, the width of the spectrum is small compared to the Larmor frequency  $\omega_0$ . If one had to acquire and record directly the  $M_{xL}(t)$  signals, the required electronics would have to be very fast in order to handle frequencies  $\omega/2\pi$  that can reach many hundreds of MHz. Since this kind of electronics is either not available or too expensive, a very elegant solution, the so-called *mixing technique* has been adopted. Its key advantage consists in *reducing* the high-frequency signals (via mixing) to low-frequency ones, while still preserving the signal's phase relationships.

The operation of a mixer (known also as *signal multiplier*) can be understood without entering into the details of its inner components, based on the following schematics:

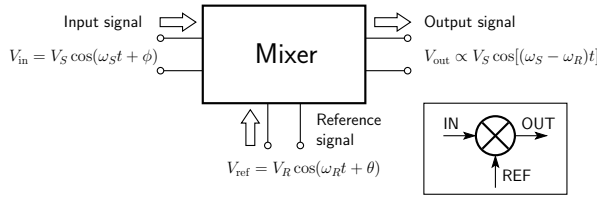


**Fig. 9** Schematic representation of a mixer used for down-converting high-frequency signals. Inset: conventional diagram of a mixer.

Here we have:

$$V_{in}(t) = V_S \cos(\omega_S t + \varphi) = V_S (\cos \varphi \cos \omega_S t - \sin \varphi \sin \omega_S t),$$

$$V_{ref}(t) = V_R \cos(\omega_R t + \vartheta). \quad (\vartheta \text{ is set by the user})$$

The output voltage,  $V_{in} \cdot V_{ref}$ , will then be:

$$V_{out}(t) = kV_S \cos[(\omega_S - \omega_R)t + \varphi - \vartheta]. \quad (61)$$

which, by choosing  $\vartheta = 0$ , becomes equivalent to  $V_{in}(t)$ :

$$V_{aus}(t) = kV_S \cos[(\omega_S - \omega_R)t + \varphi] \quad (62)$$

There is still some uncertainty whether  $\omega_S < \omega_R$  or  $\omega_S > \omega_R$ , since the cosine function does not depend on the sign of its argument.<sup>6</sup>

<sup>6</sup> This ambiguity can be removed by using another mixer where a second,  $90^\circ$  phase-shifted reference signal gives an output

$$V_{out}(t) = kV_S \sin[(\omega_S - \omega_R)t + \varphi]$$

The individual parts of the current NMR spectrometer are shown schematically in Fig. 10. Their functionality and mode of operation are described in detail in the technical manual of the spectrometer. Here we mention only about the dual role of the *oscillator*. On one hand, in *transmit* mode, the oscillator defines the frequency of the alternating magnetic field  $B_1$  during the RF pulse generation. On the other hand, in *receive* mode, the oscillator defines the frequency of the reference signal  $V_{ref}(t)$ , which is used by the mixer for down-converting the NMR FID signal.

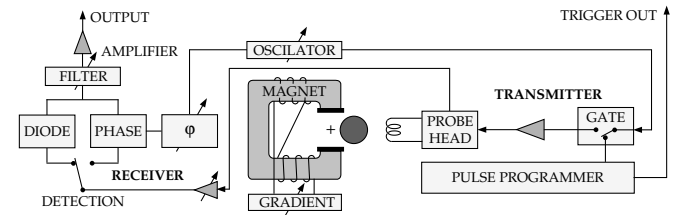


**Fig. 10** Block diagram of the NMR spectrometer.

By recording both output signals, with  $\vartheta = 0$  and  $\vartheta = -\frac{\pi}{2}$ , respectively, one can determine the sign of  $(\omega_S - \omega_R)$  as well as the phase angle  $\varphi$ . This data acquisition technique is known as *quadrature detection*.

When the two above phases can be set to the absolute  $\vartheta = 0$  and  $\vartheta = -\frac{\pi}{2}$  values, resp., then the output signal of the cosine (sine) channel will correspond to the absorption (dispersion) NMR signal.

## 9.2 Pulsed NMR methods

### 9.2.1 The spin-echo method

In many cases, the decay in time of the transverse magnetization after a  $90^\circ$  pulse is strongly influenced by magnetic field inhomogeneities, i.e., by the fact that the local magnetic field at different nuclear sites can vary considerably.

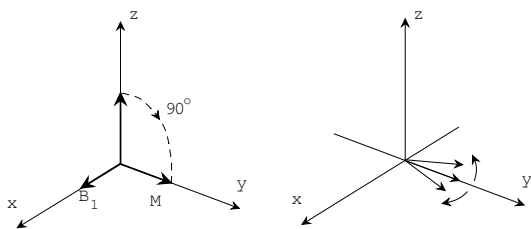


**Fig. 11** The macroscopic magnetization  $M$  after a  $90^\circ$  pulse fans-out due to inhomogeneous internal and externally-applied fields.

This field variations can have external causes, related to inhomogeneities of the applied field, but they can also reflect inner inhomogeneities, for instance, due to dipolar fields from neighbouring nuclei. After a  $90^\circ$  pulse the spins precess with slightly different frequencies and, with time, progressively de-phase. The macroscopic magnetization of the spin ensemble fans-out (Fig. 11 depicts the situation in the rotating frame) with the observable result of a decaying signal (whence the name *free induction decay*). These effects, provided they stay constant in time, can be eliminated by using the spin-echo method.

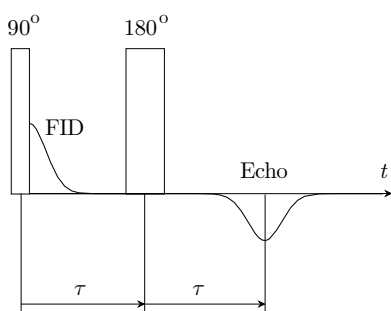


**Fig. 12** Schematic representation of a spin-echo sequence.

The basic idea behind the spin-echo method is shown in Fig. 12. At a certain time  $\tau$  after a first  $90^\circ$  pulse one applies a second  $180^\circ$  pulse. This reverts all spin orientations, which then tend to refocus. After a time  $2\tau$  from the initial pulse all spin are again in phase, i.e., the macroscopic magnetization is fully recovered and one obtains an NMR signal, the so-

called *spin-echo*. On the other hand, when at the time  $2\tau$  the nuclei being studied have left their original positions and are found in other regions of the inhomogeneous field or, when during the time  $2\tau$  the local field at a given nuclear site has changed, then the spins do not refocus any more after a spin-echo sequence. In this case, depending on the importance of such effects, one obtains only a weak echo or even no echo at all. By employing the spin-echo method it is possible to separate the interesting intrinsic effects from those trivially related to the applied-field inhomogeneities and investigate them in detail.

### 9.2.2 Inversion-recovery pulse sequence

The longitudinal spin-lattice relaxation time  $T_1$  can be easily measured by means of a simple  $180^\circ$ - $90^\circ$  inversion pulse sequence (see Fig. 13). In this case, the magnetization is initially inverted by means of a  $180^\circ$  pulse (after which there is no observable NMR signal, since  $\mathbf{M}$  does not have any transverse,  $x$ - or  $y$ -components). Next, due to the spin-lattice relaxation, the magnetization approaches its equilibrium state. When at different times  $\tau$  a  $90^\circ$  pulse (also known as detection pulse) is applied, it brings the magnetization in the  $xy$  plane and allows the observation of an NMR signal. The amplitude of the signal is proportional to the  $z$ -component of the magnetization just before the detection pulse (see Fig. 14).

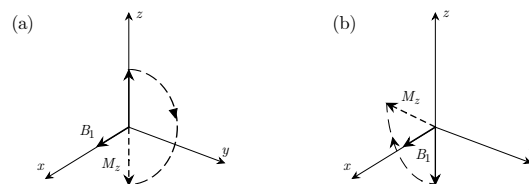


**Fig. 13** Inversion-recovery sequence: a  $180^\circ$  pulse is applied at  $t = 0$  (a), then a  $90^\circ$  detection-pulse is applied at a variable  $t = \tau$  (b).

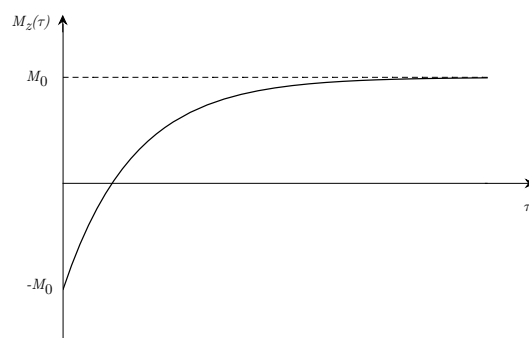


**Fig. 14** Evolution of the  $z$ -component of magnetization  $M_z(\tau)$  after applying a  $180^\circ$  pulse.

From the Bloch equations, for the  $z$ -component of magnetization one can write

$$\frac{dM_z}{dt} = \frac{M_0 - M_z}{T_1}. \quad (63)$$

By requiring that  $M_z(t = 0) = -M_0$  as an initial condition, we obtain the following solution

$$M_z(t) = M_0 \left[ 1 - 2 \exp\left(-\frac{t}{T_1}\right) \right]. \quad (64)$$

It is useful to know that  $M_z(t = 3T_1) \approx 0.95M_0$  and  $M_z(t = 5T_1) \approx 0.993M_0$ , i.e., after a time lapse of  $5T_1$  the magnetization almost fully recovers to its initial value.

## 10 Magnetic resonance imaging (MRI)

Since an RF pulse excites all the nuclei in a selected slice of the sample, the received signal is a sum of the contributions from all the spins in that slice. It is clear that, to be able to distinguish different parts of a sample, the spatial information has to be *encoded* into the NMR signal. The easiest way to achieve this, consists in using (linear) magnetic field gradients. Indeed, by applying a fixed gradient  $G_x$  during data acquisition, the information on position  $x$  is encoded into the frequency of the signal: to higher field values will correspond higher frequencies and vice versa:

$$\nu = \gamma(B_0 + xG_x) = \nu_0 + \gamma x G_x. \quad (65)$$

While in the absence of a gradient one would expect a single line, in its presence the resonance frequency will be proportional to the position of the spin. In addition, the intensity of the signal at  $x$  will depend on the concentration of nuclear spins there. Thus, tissue that contains a large amount of hydrogen, which occurs abundantly in the human body in the form of water, will produce a high intensity signal (bright image), whereas tissue that contains little or no hydrogen (e.g., bone) will appear black.

### 10.1 Back-projection imaging

This is one of the first (and simplest) forms of magnetic resonance imaging to be used. In the back-projection technique, the object is first placed in a magnetic field. Then a one-dimensional field gradient is applied at *several angles*, and an NMR spectrum is recorded for each angle. Once data has been recorded, they can be backprojected through space in computer memory (back-projection means a projection from the spectrum towards the object). Finally, the background intensity is suppressed and the artefacts are removed to obtain a 2D image of the sample's cross section. By combining several different cross sections one can create a holographic 3D

image of the body under investigation. Sometimes the back-projection scheme is called also inverse Radon transform.

Today, the sophistication of MRI is such that one can acquire images in real time, allowing one to monitor the brain activity under different conditions via the so-called *functional MRI*.

## 11 Measurement program

1. Calibrate the RF pulse width  $\pi/2$  by means of a *spin-rotation* experiment. To this purpose, follow the evolution of the FID amplitude as a function of pulse duration (in steps of  $0.5 \mu\text{s}$ ). The maximum FID amplitude is achieved when  $\alpha = \pi/2$ . What is the field value  $B_1$  corresponding to the optimal pulse length?
2. Check the NMR signal both at exact resonance, as well as slightly out of it (by changing the field  $B_0$ ). Compare the FID time signals and the respective FFT spectra. In what are they similar and in what they differ? What determines the width of the frequency spectrum?
3. By using the inversion pulse sequence, estimate the *spin-lattice* relaxation time  $T_1$  of protons in water. Note: For a reasonably fast relaxation, instead of pure water, we will use a  $6.5 \times 10^{-4} \text{ mol/l MnSO}_4$  solution containing paramagnetic  $\text{Mn}^{2+}$  ions.
4. By using the spin-echo method, estimate the *spin-spin* relaxation time  $T_2$  of protons in water. Repeat the experiment in the presence of a small field-gradient. Are the previous results still valid and why?
5. By means of the method of gradients (described in detail in App. A), estimate the self-diffusion coefficient of water molecules. To this purpose two spin-echo measurements have to be carried out. The first one using a fixed gradient  $\partial B_0/\partial z$ , but a variable delay  $\tau$  and a second one using a variable field gradient, but a fixed delay. The magnetic field gradient should preliminarily be calibrated by using a special phantom sample.
6. Calibrate the field gradient by using the phantom sample depicted in Fig. 16. Replace the phantom by a sample lacking axial symmetry and acquire the  $^1\text{H}$  NMR spectra at regular angular positions. Once the acquisition is finished, use back-projection to reconstruct the image. Does it resemble the real object? Estimate the spatial resolution of your image and consider how it can be improved.

## A Measurement of self-diffusion coefficient

As already explained in Sec. 9.2.1, inhomogeneity effects arising from the externally applied field can be eliminated by the use of the *spin-echo* method (see Fig. 12). The dependence of the echo amplitude on time  $2\tau$  is given by:

$$M(2\tau) = M_0 \exp\left(-\frac{2\tau}{T_2}\right). \quad (66)$$

However, things change when during the time  $2\tau$  the nuclei under investigation diffuse, thereby modifying their original locations. If the magnetic field inhomogeneity (i.e., the  $\partial B_0/\partial z$  gradient) is large and the nuclear diffusion strong, then the time dependence of the echo amplitude is given by the modified formula

$$M(2\tau) = M_0 \exp\left(-\frac{2\tau}{T_2}\right) \exp\left[-\left(\gamma \frac{\partial B_0}{\partial z}\right)^2 \frac{2}{3} D \tau^3\right]. \quad (67)$$

Here  $D$  denotes the diffusion coefficient, as defined from the first Fick's law (for a quick introduction to Fick's laws check the chapter on diffusion in any thermodynamics book). The derivation of Eq (67) is described in detail in App. G of Ref. [13].

If now the  $\partial B_0/\partial z$  gradient is known, one can estimate the diffusion coefficient  $D$  as the pre-factor to the  $\tau^3$  term.

## B Some technical data of NMR spectrometer

### Setting the distance between pulses:

The time distance between pulses  $\tau$  can be set by means of the two knobs shown in Fig. 15. The upper knob is used to *continuously* change the time delay via its (arbitrary) three-digit display. The lower knob instead acts as a multiplier for the value already set with the upper knob. Three possible multiplication factors are available:  $\times 1$ ,  $\times 10$ , and  $\times 100$ . As expected, the time delay depends *linearly* on the upper-knob setting. However, due to unavoidable inaccuracies, there is both a variable offset and the coefficients do not scale by an exact factor of ten. The table below reports the dependence of time delay on the knob settings.

Setting	Time delay (ms)
$\times 1$	$\tau(S) = 1.264 + 0.038 S$
$\times 10$	$\tau(S) = 12.24 + 0.392 S$
$\times 100$	$\tau(S) = 109.1 + 3.763 S$ ( $S \leq 700$ )

### Calibration of field gradient:

The magnetic field gradient  $\partial B_0/\partial z$  can be set (in arbitrary units) by means of the relevant knob. To calibrate the gradient value we will use a phantom sample made of plastic (see Fig. 16). It consists of two capillaries of 0.8 mm in diameter and 4.6 mm apart. Both capillaries are filled with silicon grease, a substance rich in hydrogen and, hence, easy to detect via  $^1\text{H-NMR}$ . When a magnetic field gradient is applied to this special sample, the hydrogen nuclei in the two capillaries will sense different fields and, consequently, will display different Larmor precession frequencies.

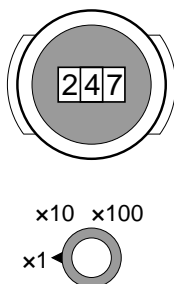


Fig. 15 Knobs to set the distance between pulses.

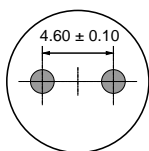


Fig. 16 Phantom sample for calibrating the magnetic field gradient.

### Frequency calibration on the LCD screen:

The time-domain NMR signals (FID and echo) are sampled at 512 equidistant intervals, digitized, and finally shown on the LCD screen of the digital oscilloscope, whose time base is set at a certain value  $T$  [s/cm]. However, not all the recorded points will be shown on the 10-cm wide LCD screen, but only the first 200 ones. The time resolution used to sample the signal is therefore:

$$\Delta t = T \frac{10}{200} [\text{s}].$$

Despite the partial display of FID, its Fourier transform is calculated using the whole time-domain signal, i.e., all the 512 sampled points. This implies a frequency resolution of

$$\Delta f = \frac{1}{512 \cdot \Delta t} [\text{Hz}].$$

From the resulting Fourier spectrum, only the first 100 frequency points will be displayed on the screen. Consequently, the required frequency calibration factor (i.e., frequency base) will be given by

$$F = \frac{100 \cdot \Delta f}{10} = \frac{200}{512} \cdot \frac{1}{T [\text{s/cm}]} [\text{Hz/cm}].$$

## C Biographic notes [17]

Edward Mills Purcell (1912–1997)

American physicist, professor at the Massachusetts Institute of Technology and Harvard University. His main domains were relaxation phenomena and magnetic properties in low temperatures.



He received the Nobel prize together with Felix Bloch “for their development of new methods for nuclear magnetic precision measurements and discoveries in connection therewith” in 1952. Besides NMR, Purcell is known also for other scientific achievements, such as the successful detection of the emission of radiation at 1421 MHz by atomic hydrogen in the interstellar medium. Each of these fundamental discoveries has led to an extraordinary range of developments. NMR, for example, initially conceived as a way to reveal properties of atomic nuclei, became a major tool for research in material sciences, chemistry, and even medicine, where magnetic resonance imaging (MRI) is now an indispensable tool. Radio spectroscopy of atoms and molecules in space, following from the detection of the hyperfine transition in hydrogen as the first example, has become a major part of the ever-expanding field of radio astronomy.

Purcell made also contributions in biophysics, astronomy, etc. He was a very influential teacher and a valued advisor and consultant throughout his professional life.

Felix Bloch (1905–1983)

Bloch was born in Zurich, Switzerland, and was educated at the Federal Institute of Technology and at the University of Leipzig, where he obtained his PhD in 1928. He taught briefly in Germany and in 1933 moved to America, via various institutions in Italy, Denmark, and Holland. In 1934 he joined the Stanford staff, remaining there until his retirement in 1971 and serving from 1936 onward as professor of physics. He also served briefly as first director of CERN in Geneva.

In 1946, Bloch and Edward Purcell independently introduced the technique of nuclear magnetic resonance (NMR). This was used initially to determine the magnetic moment of protons, but later on it developed into a powerful tool for the analysis of the more complex molecules of organic chemistry. In 1952 Bloch shared the Nobel Prize for physics with Purcell for their work on NMR.



Bloch worked extensively in the field of solid-state physics developing a detailed theory of the behaviour of electrons in crystals and revealing much about the properties of ferromagnetic domains. He contributed also to the domains of superconductivity, quantum electrodynamics and the physics of neutrons.

## References

1. A. Abragam, *The Principles of Nuclear Magnetism* (Oxford University Press, Oxford, 1961).
2. P. Callaghan, *Principles of Nuclear Magnetic Resonance Microscopy* (Oxford University Press, Oxford, 1994).
3. B. Cowan, *Nuclear Magnetic Resonance and Relaxation* (Cambridge University Press, Cambridge, 2005).
4. E. Fukushima, S. B. W. Roeder, *Experimental Pulse NMR* (Addison-Wesley, Reading, MA, 1981).
5. J. P. Hornak, *The Basics of MRI*. Online course at <http://www.cis-rit.edu/htbooks/mri/index.html> (Feb. 2014).
6. J. Keeler, *Understanding NMR Spectroscopy*, 2nd ed. (John Wiley & Sons, Chichester, 2010).
7. M. H. Levitt, *Spin Dynamics: Basics of Nuclear Magnetic Resonance*, 2nd ed. (John Wiley & Sons, New York, 2008).
8. R. S. Macomber, *A Complete Introduction to Modern NMR Spectroscopy* (Wiley-Interscience, New York, 1998).
9. P. A. Rinck, *Magnetic Resonance*, 7th ed. Online course at <http://www.magnetic-resonance.org/> (Feb. 2014).
10. A. C. Melissinos, *Experiments in Modern Physics* (Academic Press, New York, 1966), ch. 7.
11. G. E. Pake, T. L. Estle, *The Physical Principles of Electron Paramagnetic Resonance*, 2nd ed. (Benjamin, Reading, MA, 1973).
12. D. Preston and E. Dietz, *The Art of Experimental Physics* (Wiley, New York, NY, 1991), pp. 264–285.
13. C. P. Slichter, *Principles of Magnetic Resonance*, 3rd ed. (Springer, Berlin, 1996), ch. 11.
14. D. Shaw, *Fourier Transform Spectroscopy* (Elsevier, Amsterdam, 1976).
15. G. Shatz, A. Weidiger, M. Deicher, *Nukleare Festkörperphysik*, 4. Aufl. (Vieweg + Teubner, Wiesbaden, 2010).
16. D. D. Traficante, “NMR Concepts”, in Martha D. Bruch ed., *NMR Spectroscopy Techniques*, 2nd ed., Practical Spectroscopy, Vol. 21 (Marcel Dekker, New York, 1996) Chap. 1.
17. J. Daintith and D. Gjersten eds., *A Dictionary of Scientists* (Oxford University Press, Oxford, 1999).